

Peculiar thermal behavior of UO₂ local structure

Prieur, D.; Epifano, E.; Dardenne, K.; Rothe, J.; Hennig, C.; Scheinost, A.; Neuville, D.;
Martin, P.;

Originally published:

November 2018

Inorganic Chemistry 57(2018)23, 14890-14894

DOI: <https://doi.org/10.1021/acs.inorgchem.8b02657>

Perma-Link to Publication Repository of HZDR:

<https://www.hzdr.de/publications/Publ-27658>

Release of the secondary publication
on the basis of the German Copyright Law § 38 Section 4.

PECULIAR THERMAL BEHAVIOR OF UO₂ LOCAL STRUCTURE

D. Prieur^{1,2,3*}, E. Epifano⁴, K. Dardenne⁵, J. Rothe⁵, C. Hennig^{1,2}, A. C. Scheinost^{1,2}, D. R. Neuville⁶, P. M. Martin³

Most materials expand in one, two or all three dimensions with temperature because of the anharmonicity of lattice vibration, and only few behave in the opposite way, *i.e.* shrink with increasing temperature¹. Uranium dioxide, whose thermal properties are of significant importance for the safe use of the nuclear energy², was considered for a long time to belong to the first group from room temperature to the melting point at 3147 ± 20 K^{3,4,5}. This view was challenged by recent *in situ* synchrotron X-ray diffraction measurements, showing an unusual thermal decrease of the U-O distances up to the melting point⁶. This thermal shrinkage was interpreted as a consequence of the splitting of the U-O distances due to a change in the U local symmetry from *Fm-3m* to *Pa-3*⁷. In contrast to these previous investigations and using an element-specific synchrotron-based spectroscopic method, we show here that the U sublattice remains locally of the fluorite type from 50 K to 1265 K, and that the decrease of the first U-O bond lengths with increasing temperature is associated to an increase of the disorder, which we modelled using the Einstein model. These findings are of significant importance in order to predict the thermal behaviour of nuclear fuel, as well as to understand the accumulation of fission product in the nuclear fuel.

UO₂ is used in many countries as nuclear fuel for electrical power generation⁸. Both, its thermophysical and thermal properties at high temperatures are critical for the safe operation of nuclear reactors, as has been sadly demonstrated by the nuclear accidents of Chernobyl and Fukushima⁹.

Under ambient temperature, neutron diffraction has shown that UO₂ crystallizes in the fluorite structure (CaF₂)¹⁰: the uranium cations form a face-centred cubic lattice in which all the tetrahedral sites are occupied by oxygen anions¹¹. In this *Fm-3m* symmetry, each uranium atom is surrounded by eight oxygen atoms at 2.37 Å and twelve second neighbour uranium atoms at 3.87 Å. The thermal behaviour of the UO₂ structure has been studied for decades notably by *in situ* x-ray and neutron diffraction showing that the fluorite structure is maintained and that its lattice parameter expands^{4,5,2,12}. Considering the *Fm-3m* symmetry, one expects that the first U-O and U-U distances are proportional to the lattice parameter. At high temperature, UO₂ can no longer be described as a perfect fluorite structure with harmonic thermal vibrations of U and O on their respective sites: It was first erroneously attributed to relaxation of anions from their room temperature positions ($\frac{1}{4}, \frac{1}{4}, \frac{1}{4}$) to positions with slightly different coordinates ($\frac{1}{4}+\delta, \frac{1}{4}+\delta, \frac{1}{4}+\delta$)¹³. The thermal evolution was later reproduced by including third cumulant coefficients which account for the anisotropic anharmonic thermal motion of the oxygen atoms remaining at the fluorite position ($\frac{1}{4}, \frac{1}{4}, \frac{1}{4}$)¹⁴.

Several diffraction measurements at *circa* 1300 K showed a thermal increase of the U-O distances as well as of the unit cell^{13,15,16}. In contrast, more recent synchrotron X-ray diffraction measurements by Skinner *et al.*⁶ contradict these observations. Indeed, the corresponding atomic pair-distribution function (PDF) results indicate that the first U-O bond length contracts on heating up to the melting point (3147 ± 20 K³) whereas the inter metal distance expands. It is assumed that the U-O contraction results from the existence of atomic disorder in the anion lattice. Subsequent neutron PDF results obtained by Desgranges *et al.*⁷ also support the shortening of the U-O bonds as a consequence of the splitting of the O shell leading to two U-O distances, instead of one in the fluorite structure. Hence, these measurements also showed that with the temperature the local symmetry around U changes from *Fm-3m* to *Pa-3*.

From this short review, one can see that discrepancies exist on both the local symmetry of UO₂ at high temperature and the thermal behaviour of the U-O distances. Here, we use *in situ* X-ray Absorption Fine

¹ Helmholtz-Zentrum Dresden-Rossendorf, Institute of Resource Ecology, P.O. Box 10119, 01314 Dresden, Germany. ² Rossendorf beamline (BM20-CRG), European Synchrotron Radiation Facility, 6 rue Jules Horowitz, BP 220, 38043 Grenoble, France. ³ Former address: European Commission, Joint Research Centre (JRC), Postfach 2340, 76125 Karlsruhe, Germany. ⁴ CEA, Nuclear Energy Division, Research Department on Mining and Fuel Recycling Processes, SFMA, BP 17171, F-30207 Bagnols-sur-Cèze, France. ⁵ Karlsruhe Institute of Technology, Institute for Nuclear Waste Disposal (KIT-INE), Hermann-von-Helmholtz-Platz 1, D-76344 Eggenstein-Leopoldshafen, Germany. ⁶ Géomatériaux, Institut de Physique du Globe de Paris-CNRS, USPC 1 rue Jussieu, 75005 Paris, France. .

* Corresponding author: d.prieur@hzdr.de

Structure (XAFS) spectroscopy to tackle this discrepancy, by following the local structure around U in UO_2 as a function of temperature from 50 K to 1300 K.

In situ X-ray Absorption Near Edge Spectroscopy (XANES) and Extended X-ray Absorption Fine-Structure (EXAFS) measurements were conducted at the ROBL beamline¹⁷ (ESRF) and at the INE beamline¹⁸ (ANKA). The XAFS spectra from 50 K to 150 K were collected at ROBL using a cryostat at the U L_{II} edge on UO_2 samples that have been previously sintered in Ar-4% H_2 at 2023 K during 4 hours¹⁹. Based on UO_2 thermodynamics²⁰, these heating conditions ensure a stoichiometric oxide. The XAS measurements from RT to 1300 K were recorded at INE-BL at the U L_{III} edge with a dedicated furnace on a fragment extracted from the same dense (98%) sintered $\text{UO}_{2.00}$ pellet used at ROBL. The furnace atmosphere was held constant in Ar-4% H_2 to maintain the stoichiometry.

Comparing the collected XANES spectra with a $\text{UO}_{2.00}$ reference measured at 298 K on both beamlines^{21,22}, we observe that our investigated UO_2 remains stoichiometric independently of the temperature (Figure 1). Any deviation from the stoichiometry of the compound would be identifiable from U $L_{II,III}$ XANES by a shift of the white line toward lower (*i.e.* reduction) or higher (*i.e.* oxidation) energy^{19,21-24}. One should note that, contrary to the previous above-mentioned investigations on UO_2 , this direct measurement of the U oxidation state ensures that the acquired data really refer to a stoichiometric compound.

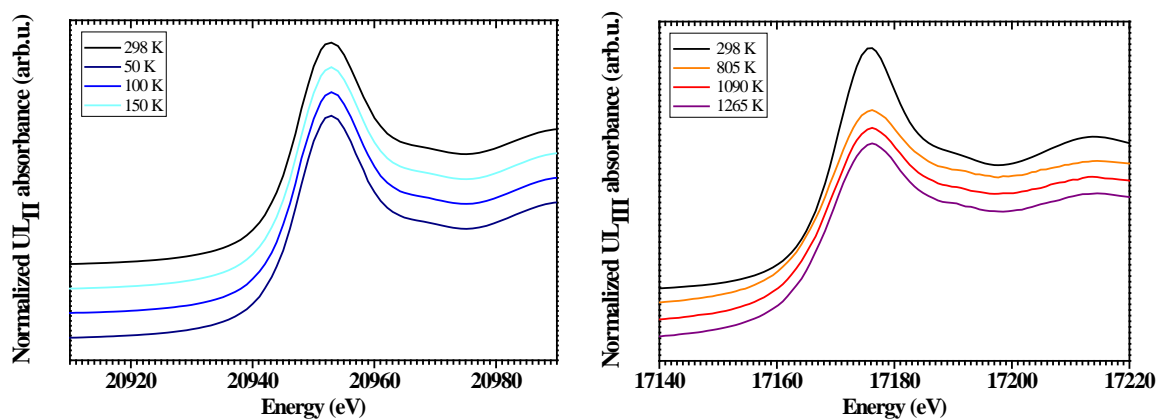


Figure 1: XANES spectra of stoichiometric UO_2 . (Left) UL_{II} XANES spectra of $\text{UO}_{2.00}$ at 50K, 100K, 150K and 298K²¹. (Right) UL_{III} XANES spectra of $\text{UO}_{2.00}$ at 298K²², 805K, 1090K and 1265K.

While heating from 50 K to 1265 K, no strong modification of the local environment can be observed in the experimental EXAFS spectra (Figure 2). The main visual evolution is a damping of the EXAFS oscillations, especially at high k -values, due to the increase of the thermal vibration. For this reason, only the first U-O bond lengths have been fitted for each EXAFS spectrum.

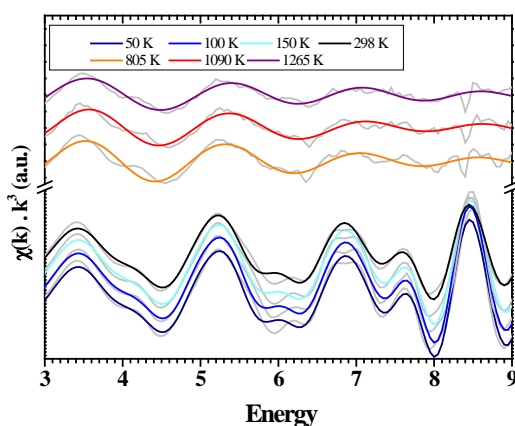


Figure 2: EXAFS spectra of stoichiometric UO_2 . Fitted and experimental k^3 -weighted EXAFS spectra of $\text{UO}_{2.00}$ collected at several temperatures. The experimental data are in light grey and the data fitted with the $Fm\text{-}3m$ space group are coloured. Note that for the temperatures 50K, 100K and 150K, the EXAFS spectra were collected at the UL_{II} edge.

Taking into account the findings of Skinner *et al.*⁶ and Desgranges *et al.*⁷, each EXAFS spectrum has been fitted independently of the temperature using both *Fm-3m* and *Pa-3* structural models.. In the former, the first anion shell is composed of eight equidistant oxygen atoms ($r_{\text{U-O}} = 2.37 \text{ \AA}$) while in the latter the UO_8 polyhedron is a distorted oxygen cube with six shorter distances ($r_{\text{U-O}} = 2.34 \text{ \AA}$) and two longer ($r_{\text{U-O}} = 2.56 \text{ \AA}$)⁷. Note that neither clustering of oxygen interstitials (*i.e.* Willis or cubo-octahedral clusters) nor shorter U-O distances have been observed, the latter having already being reported in UO_{2+x} phases²⁵. For all temperatures, the best refinements are achieved using a *Fm-3m* structural model. Even if the fit residuals value is rather good, the derived crystallographic parameters derived from the *Pa-3* symmetry are very far off from the values determined by Desgranges and seem not to be reasonable. As an example, the *Pa-3* EXAFS-derived structural parameters of the UO_2 samples heated at 1275 K are given in the Table 1. One can note that close values of the residual factors are obtained with both models. However, the fitted Debye-Waller factors are extremely high ($>0.025 \text{ \AA}^2$) in the case of *Pa-3* and more importantly the distances do not converge toward the model values. On the contrary they diverge from reasonable values for a distorted UO_8 polyhedron. Contrary to the work of Desgranges *et al.*⁷, our experimental data indicate that the local *Fm-3m* symmetry remains and no thermal transition occurs toward the lower *Pa-3* symmetry. The present results do not support a local change of space group with temperature. One of the reasons that could explain this discrepancy is a difference of stoichiometry of the studied compounds. Indeed, the UO_{2+x} solid solution is known to have a large hyperstoichiometric domain for temperatures above 600K. Moreover, several other phases with different crystal structures exist in the U-O phase diagram, depending on the temperature and the stoichiometry²⁰. The latter is notably very sensitive to the oxygen partial pressure during the experimental treatment. In this study, the measurements were carried out in Ar- 4 % H_2 while the neutron diffraction data of Desgranges *et al.*⁷ were collected using a container sealed under vacuum. In principle, that configuration should not lead to an (appreciable) oxidization from $\text{UO}_{2.00}$ to UO_{2+x} , but no experimental measurement of the stoichiometry was performed to confirm this assumption. On the contrary, here we used XANES, which is a direct, powerful and acknowledged technique^{19,21-24}, to derive the uranium oxidation states and to ensure that UO_2 remains stoichiometric and that no UO_{2+x} phase was formed during the thermal treatment.

Table 1: Structural parameters. The interatomic distances, the coordination numbers and the Debye-Waller factors were derived from the EXAFS spectra at 1265 K using either a *Fm-3m* or *Pa-3* structural model. For the *Pa-3* fitting, the coordination numbers were fixed to the theoretical values as otherwise no convergence was achieved. The uncertainties are the numbers in bracket.

| Structural parameters | <i>Fm-3m</i> | <i>Pa-3</i> | |
|-------------------------------|--------------|-------------|-----------|
| R (\AA) | 2.343 (6) | 2.29 (1) | 2.73 (1) |
| N | 7.5 (1.2) | 6 | 2 |
| σ^2 (\AA^2) | 0.017 (3) | 0.025 (5) | 0.025 (5) |
| R_f ($\times 10^{-3}$) | 8 | 12 | |

The interatomic distances, the coordination numbers and the Debye-Waller factors were then derived for each temperature by fitting all the EXAFS spectra with a *Fm-3m* structure (Figure 3). From 50 K to 298 K, no significant variation of the structural parameters has been noted. For these temperature, the UO_8 polyhedron is composed of one uranium atom neighbored by 8.0 (5) oxygen anions at 2.358 \AA . While heating from 298 K to 1265 K, significant variations of these crystallographic parameters are observed. There is a decrease of the first U-O bond length, which is quantitatively and qualitatively in good agreement with the neutron measurements of Skinner *et al.*⁶ (Figure 3 Top right). Although within the error bar, the coordination seems to drop as well, which again would agree with Skinner *et al.*⁶ who reported a value of 6.7 (5) at 3270 K. However, based on molecular dynamic simulation²⁶, they also argue that the coordination number should essentially have a constant value of 8 up to the melting point and that, only then, there is a rearrangement toward $\text{UO}_{6.7(5)}$ polyhedron. Considering the error bar on our EXAFS-derived coordination numbers, we can't confirm nor exclude this proposed mechanism. We can only say that our results suggest that there is already below the melting point a rearrangement of the oxygen coordination shell around uranium, which indeed would be supported by the observed contraction of the first U-O distances. In addition, we observed an increase of the Debye-Waller factors, which corresponds to the parallel mean square relative displacement and parametrizes the

variance of the distance distribution. In other terms, it accounts for the effects of structural and vibrational disorder. In our case, the observed increase of the Debye-Waller factor can mainly be attributed to the vibrational disorder, as the static contribution seldom exhibits temperature dependence²⁷. This disorder is likely due to the displacement of the oxygen anions from their native sites. In that case, a monotonic increase with temperature is expected, as in our case for temperatures ranging from 600 K to 1265 K²⁸. Our experimental values were satisfactorily fitted using the Einstein model²⁹ and an Einstein temperature of 480 ± 20 K was found, which is slightly lower than earlier reported values, i.e. 542 K³⁰ and 620 K¹⁶.

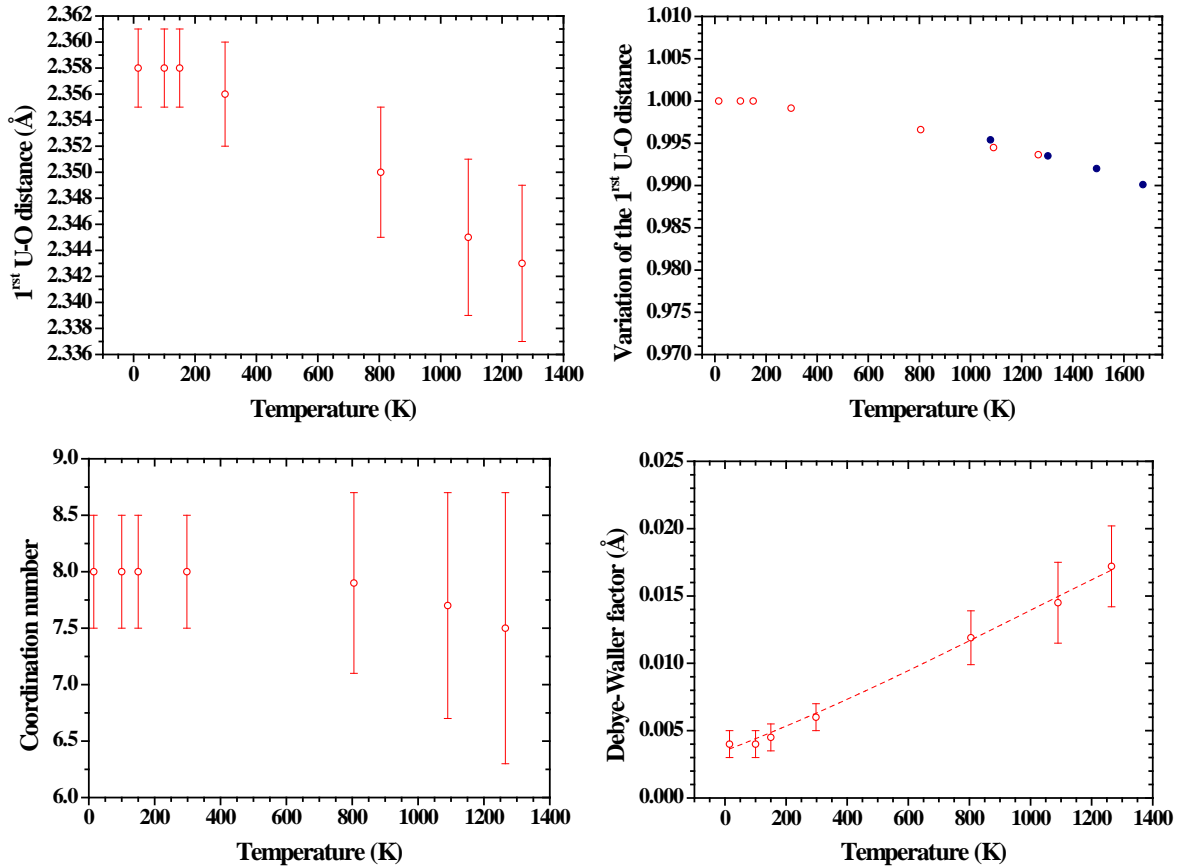


Figure 3: Temperature dependence of the EXAFS derived structural parameters of stoichiometric UO_2 . (Top left) The 1st U-O fitted distances as a function of the temperature. (Top right) The 1st U-O fitted distances of stoichiometric UO_2 are normalized to the 15K value and compared to the experimental data of Skinner *et al.*⁶, which are represented with blue circles. (Bottom left) The coordination number of the 1st O shell as a function of the temperature. (Bottom right) The Debye-Waller factors derived from the EXAFS analysis of the 1st U-O distances are plotted as a function of the temperature (red open circle). These have been fitted using the Einstein model (red straight line) and the calculated Einstein temperature is $\theta_E = 480 \pm 20$ K.

As the majority of operating nuclear reactors are fuelled with UO_2 , demonstrating and quantifying the contraction of the local UO_2 structure with the temperature is an essential ingredient in assessing the safety relevant behaviour of this material. Indeed, current calculation codes are only based on the expansion of the whole lattice, *i.e.* both interatomic distances and unit cell. These same theoretical models are used notably to predict the behaviour of the fuel in normal and off-conditions. However, our present results clearly show that one cannot assume that the anionic interatomic distances expand with the temperature. On the contrary, they contract, which means that the overall volume of the interstitial sites decreases. Consequently, our current understanding of the accommodation of fission products in the UO_2 structure needs deeper consideration to enable even better understanding of the operation safety of UO_2 nuclear fuel.

METHODS

XAS data acquisition

The XAS spectra from 15K to 150 K were recorded at the ROBL beamline (ESRF, Grenoble, France) under dedicated operating conditions (6.0 GeV, 170-200 mA). Double crystal monochromator mounted with Si (111) crystals were used. Samples were held at 15K, 100 and 150K using a closed-cycle helium cryostat. Data were collected in both transmission and fluorescence modes at the uranium L_{II} (20948 eV) edge. Fluorescence signal was measured with a 13-element Ge solid state detector using a digital amplifier.

The XAS measurements from RT to 1265K were conducted at the INE-Beamline of the KIT synchrotron light source (Karlsruhe Institute of Technology, Germany). The storage ring operating conditions were 2.5 GeV and 100-160mA. A Ge [422] double crystal monochromator coupled with collimating and focusing Rh-coated mirrors was used. XAS spectra were collected at various temperatures in fluorescence mode at the U L_{III} edge (17166 eV) with a five-element germanium solid-state detector. Energy calibration was achieved by measuring the K XANES spectrum of a Y reference foil (17038 eV) located between the second and third ionization chambers. The measurements were conducted on a fragment of a UO_{2,00} pellet that has been previously sintered in Ar-4% H₂ at 2023 K during 4h. Prior measurement, the sample is mechanically fixed on a Pt/Ir (90/10) wire. This heating element is then inserted into a dedicated furnace which allows collecting in situ XAS data on radioactive samples in various atmospheres and up to 2000 K.

The present data have been collected in Ar-4% H₂ at 298, 805, 1090 and 1265 K. During each of these successive temperature plateaus, 4 U L_{III} EXAFS scans have been collected. Note that the Pt/Ir wire temperature was calibrated before the measurement.

In situ XAS

A complete review of the heating wire can be found in Neuville *et al.*³¹. The heating wire is just a platinum or alloy wire with a diameter between 1 and 2 mm, flattened in the middle with a hole with a diameter from 100 micron up to 1mm. This hole corresponds to the hot spot. This heating system has low thermal inertia and it is possible to change the temperature between room temperature up to temperatures >1600 °C in few seconds. At temperature the heating system is relatively stable and can stay at the selected temperature as long as needed during the experiments.

XAS data analysis

The XANES spectra have been normalized using linear functions for pre- and post- edge modelling. The white-line maxima have been taken as the first zero-crossing of the first derivative. Pre-edge removal, normalization and self-absorption correction were performed using the ATHENA software³².

The EXAFS oscillations, collected up to 14 Å⁻¹, were extracted from the raw absorption spectra with the ATHENA software³² and Fourier-transformed using a Hanning window over the k₂-range [3-9] Å⁻¹. Phases and amplitudes for the interatomic scattering paths were calculated with the *ab initio* code FEFF 8.40³³. Both *Fm-3m* and *Pa-3* symmetries have been used as structural models in the FEFF calculations to fit the EXAFS spectra. In the former space group, the first anion shell is composed of eight equidistant oxygen atoms while in the latter the UO₈ polyhedron is a distorted oxygen cube with two longer and six shorter distances. The amplitude factor (S_0^2) was set at 0.90. The shift in the threshold energy (ΔE_0) was varied as a global parameter.

REFERENCES

1. Withers, N. Thermal expansion: Shrinking stuff. *Nature Chemistry* (2009). doi:10.1038/nchem.508
 2. Guéneau, C., Chartier, A. & Van Brutzel, L. 2.02 - Thermodynamic and Thermophysical Properties of the Actinide Oxides. in *Comprehensive Nuclear Materials* (ed. Konings, R. J. M.) 21–59 (Elsevier, 2012). doi:10.1016/B978-0-08-056033-5.00009-4
-

3. Manara, D., Ronchi, C., Sheindlin, M., Lewis, M. & Brykin, M. Melting of stoichiometric and hyperstoichiometric uranium dioxide. *J. Nucl. Mater.* **342**, 148–163 (2005).
 4. Martin, D. G. The thermal expansion of solid UO₂ and (U, Pu) mixed oxides — a review and recommendations. *J. Nucl. Mater.* **152**, 94–101 (1988).
 5. Fink, J. K. Thermophysical properties of uranium dioxide. *J. Nucl. Mater.* **279**, 1–18 (2000).
 6. Skinner, L. B. *et al.* Molten uranium dioxide structure and dynamics. *Science* **346**, 984–987 (2014).
 7. Desgranges, L. *et al.* What Is the Actual Local Crystalline Structure of Uranium Dioxide, UO₂? A New Perspective for the Most Used Nuclear Fuel. *Inorg. Chem.* **56**, 321–326 (2017).
 8. Olander, D. Nuclear fuels – Present and future. *J. Nucl. Mater.* **389**, 1–22 (2009).
 9. Konings, R. J. M., Wiss, T. & Beneš, O. Predicting material release during a nuclear reactor accident. *Nature Materials* (2015). doi:10.1038/nmat4224
 10. Willis, B. T. M. Neutron Diffraction Studies of the Actinide Oxides. I. Uranium Dioxide and Thorium Dioxide at Room Temperature. *Proc. R. Soc. Lond. Ser. Math. Phys. Sci.* **274**, 122–133 (1963).
 11. Willis, B. T. M. Positions of the Oxygen Atoms in UO₂. *Nature* **197**, 755–756 (1963).
 12. Guthrie, M. *et al.* Thermal expansion in UO₂ determined by high-energy X-ray diffraction. *J. Nucl. Mater.* **479**, 19–22 (2016).
 13. Willis, B. T. M. Structures of UO₂, UO_{2+x} and U₄O₉ by neutron diffraction. *J Phys Fr.* **25**, 431–439 (1964).
 14. Willis, B. T. M. & Hazell, R. G. Re-analysis of single-crystal neutron-diffraction data on UO₂ using third cumulants. *Acta Crystallogr. A* **36**, 582–584 (1980).
 15. Albinati, A., Cooper, M. J., Rouse, K. D., Thomas, M. W. & Willis, B. T. M. Temperature dependence of the atomic thermal displacements in UO₂: a test case for the Rietveld profile-refinement procedure. *Acta Crystallogr. A* **36**, 265–270 (1980).
 16. Ruello, P. *et al.* Heat capacity anomaly in UO₂ in the vicinity of 1300K: an improved description based on high resolution X-ray and neutron powder diffraction studies. *J. Phys. Chem. Solids* **66**, 823–831 (2005).
 17. Matz, W. *et al.* ROBL – a CRG beamline for radiochemistry and materials research at the ESRF. *J. Synchrotron Radiat.* **6**, 1076–1085 (1999).
 18. Rothe, J. *et al.* The INE-Beamline for actinide science at ANKA. *Rev. Sci. Instrum.* **83**, 043105 (2012).
 19. Prieur, D. *et al.* Comparative XRPD and XAS study of the impact of the synthesis process on the electronic and structural environments of uranium-ameridium mixed oxides. *J. SOLID STATE Chem.* **230**, 8–13 (2015).
-

20. Guéneau, C., Baichi, M., Labroche, D., Chatillon, C. & Sundman, B. Thermodynamic assessment of the uranium–oxygen system. *J. Nucl. Mater.* **304**, 161–175 (2002).
21. Prieur, D. *et al.* Local Structure and Charge Distribution in Mixed Uranium-Amercium Oxides: Effects of Oxygen Potential and Am Content. *Inorg. Chem.* **50**, 12437–12445 (2011).
22. Martel, L. *et al.* Structural Investigation of Uranium-Neptunium Mixed Oxides Using XRD, XANES, and ¹⁷O MAS NMR. *J. Phys. Chem. C* **118**, 27640–27647 (2014).
23. Boehler, R. *et al.* Recent advances in the study of the UO₂-PuO₂ phase diagram at high temperatures. *J. Nucl. Mater.* **448**, 330–339 (2014).
24. Smith, A. L. *et al.* Structural Properties and Charge Distribution of the Sodium Uranium, Neptunium, and Plutonium Ternary Oxides: A Combined X-ray Diffraction and XANES Study. *Inorg. Chem.* **55**, 1569–1579 (2016).
25. Conradson, S. D. *et al.* Local Structure and Charge Distribution in the UO₂-U₄O₉ System. *Inorg. Chem.* **43**, 6922–6935 (2004).
26. Yakub, E., Ronchi, C. & Staicu, D. Molecular dynamics simulation of premelting and melting phase transitions in stoichiometric uranium dioxide. *J. Chem. Phys.* **127**, 094508 (2007).
27. Fornasini, P. & Grisenti, R. On EXAFS Debye-Waller factor and recent advances. *J. Synchrotron Radiat.* **22**, 1242–1257 (2015).
28. Annamareddy, A. & Eapen, J. Disorder and dynamic self-organization in stoichiometric UO₂ at high temperatures. *J. Nucl. Mater.* **483**, 132–141 (2017).
29. Sevillano, E., Meuth, H. & Rehr, J. J. Extended x-ray absorption fine structure Debye-Waller factors. I. Monatomic crystals. *Phys. Rev. B* **20**, 4908–4911 (1979).
30. IAEA. Thermodynamic and Transport Properties of Uranium Dioxide and Related Phases.
31. Henderson, G., Neuville, D. & Downs, R. *Spectroscopic Methods in Mineralogy and Material Sciences*. (De Gruyter, 2014). doi:10.1515/9781614517863
32. Ravel, B. & Newville, M. ATHENA, ARTEMIS, HEPHAESTUS: data analysis for X-ray absorption spectroscopy using IFEFFIT. *J. Synchrotron Radiat.* **12**, 537–541 (2005).
33. Rehr, J. J., Kas, J. J., Vila, F. D., Prange, M. P. & Jorissen, K. Parameter-free calculations of X-ray spectra with FEFF9. *Phys. Chem. Chem. Phys. PCCP* **12**, 5503–5513 (2010).

ACKNOWLEDGMENT

The authors acknowledge both ESRF and the KIT synchrotron light source for provision of beamtime. The authors are also entitled to both ROBL and INE teams for their help during the measurements.

AUTHOR CONTRIBUTION

P. M. M. and D.N. designed the experiment. D. P., P. M. M., D. N. and E. P. performed all the experimental work. K. D., J. R., C. H. and A. C. S. were the INE and ROBL scientists during the beamtime. D. P. and P. M. M. analysed the data. D. P. and P. M. M. wrote the manuscript.
